Original paper

Molecular profile of parathyroid tissues and tumours: a heterogeneous landscape

Romans Uljanovs[1], Ilze Strumfa[1], Guntis Bahs[1], Liga Vidusa[1], Kristine Merkurjeva[1], Ivanda Franckevica[1], Boriss Strumfs[2]

[1]Riga Stradins University, Riga, Latvia
[2]Latvian Institute of Organic Synthesis, Riga, Latvia

Advances in laboratory diagnostics and surgical treatment of primary hyperparathyroidism have ensured solid basis for research in parathyroid pathology in order to specify key molecules in pathogenesis and morphological diagnostics of difficult cases. The aim of this study was to assess the molecular landscape and its heterogeneity in primary parathyroid hyperplasia (PPH) and adenoma, compared to carcinoma and normal glands. In a retrospective analysis of 179 surgically removed parathyroid glands (102 adenomas; 27 PPH; 45 normal glands; 5 carcinomas), expression of Ki-67, p21, p27, p53, cyclin D1, Bcl-2 protein, vimentin, cytokeratin (CK) 19, E-cadherin, CD56, CD44 and parafibromin was detected by immunohistochemistry, followed by computer-assisted assessment of mean values and heterogeneity measures. Descriptive statistics and Kruskal-Wallis test were applied. Significant differences were disclosed regarding the mean and highest fraction of Ki-67 (both $p < 0.001$), p21 (both $p < 0.001$), cyclin D1 ($p = 0.002$) and p27-expressing cells ($p = 0.010$). Proliferative lesions (PPH, adenoma and carcinoma) showed statistically significantly up-regulated CK19 ($p = 0.012$), decreased E-cadherin levels and distinctive patterns of vimentin. CD44, CD56 and p53 were almost absent from parathyroid tissues. All carcinomas lacked parafibromin contrasting with invariable positivity in adenomas. Remarkable heterogeneity of cell cycle markers and intermediate filaments must be accounted for in scientific studies and elaboration of diagnostic cut-offs.

Key words: primary parathyroid hyperplasia, parathyroid adenoma, proliferation, parafibromin, heterogeneity.

Introduction

Primary hyperparathyroidism, defined as autonomous overproduction of parathyroid hormone (PTH), represents the third most common endocrine disorder. The diagnostic paradigm of primary hyperparathyroidism has shifted significantly from clinically based suspicion in symptomatic patients to almost incidental finding [1, 2] via routine biochemical laboratory assessment of serum calcium and parathyroid hormone levels. Not infrequently, the testing is initially triggered by another condition. The most frequent cause of primary hyperparathyroidism is parathyroid adenoma comprising 80-85% of cases; followed by primary parathyroid hyperplasia, found in 10-15% patients and the few cases of parathyroid carcinoma, affecting less than 1% of patients diagnosed with primary hyperparathyroidism [2, 3]. Surgery is increasingly used for the treatment of primary hyperparathyroidism, because it is the only curative

treatment [1, 4] and is considered safe [1, 2]. Consequently, pathologists have wider access to parathyroid samples. Although the diagnostics of parathyroid pathologies is significantly facilitated by preoperative imaging and intraoperative assays [2], the morphological distinction between hyperplasia *versus* adenoma, or adenoma *versus* carcinoma occasionally still remains complicated. Detailed molecular studies can identify diagnostic markers or characteristic patterns as well as highlight the pathogenesis.

Currently, medicine benefits from the golden age in parathyroid surgery. Major improvements have been achieved since the beginning of the 20th century. The surgical techniques have been elaborated in detail, defining the key structures and steps of operation and thus limiting the risk of complications. The two main approaches [2] include the classic bilateral neck exploration *versus* minimally invasive parathyroidectomy (PTE) which, in turn, embraces directed PTE, endoscopic PTE (total endoscopic, or video-assisted or robotic PTE) and isotope-guided PTE. The indications and contraindications for surgery have been specified. The preoperative diagnostics, the laboratory tests and imaging modalities ensure reliable basis to select the most appropriate surgical treatment. Currently, radiological investigations for localisation studies encompass broad spectrum of available technologies: neck ultrasound, computed tomography (CT), ^{99m}Tc-sestamibi scan, positron emission tomography-computed tomography PET/CT (using ^{18}F-fluorodeoxyglucose or ^{18}F-fluorocholine as tracers) and single-photon emission computed tomography SPECT in combination with CT [1]. Intraoperative adjunct tests, especially intraoperative assessment of PTH, support decision making during surgery. The risk of most serious complications, namely, permanent hypocalcaemia and injury of recurrent laryngeal nerve, is as low as 1-2% and below 1%, respectively [2].

Despite the multiple recent developments and undoubted benefits of parathyroid surgery, the future can present certain challenges. The Western population is aging, and primary hyperparathyroidism is known to occur more frequently in elderly patients. Thus, primary hyperparathyroidism in octogenarians and nonagenarians will become an increasingly important clinical problem [5]. Concomitant diseases can limit the application of surgery in these patients urging to offer an alternative medical approach. However, the available scope of non-surgical methods is scant. The current medical treatment is targeted towards improving bone structure and decreasing hypercalcemia. Bisphosphonates, oestrogens and selective oestrogen receptor modulators are prescribed to increase bone mineral density. Calcimimetics such as cinacalcet increase the sensitivity of parathyroid calcium-sensing receptors to extracellular calcium, thereby reducing serum calcium levels [2]. However, the effect on PTH level is only partial [6, 7], and PTH is thought to contribute directly (in parallel with hypercalcemia) to the development of vascular complications in hyperparathyroidism, such as arterial hypertension, atherosclerosis, cardiac arrhythmias, left ventricular hypertrophy, insulin resistance and diabetes mellitus [4]. Better understanding of the underlying molecular mechanisms enables highlighting pathways to targeted treatment.

In addition, postoperative histology can modify the follow-up, e.g., to determine cure. Considering that 6-month-long surveillance [2] might be resource-intensive and costly, criteria for early identification of cured patients have been proposed. These include pathologic diagnosis of a single adenoma, along with concordant imaging and intraoperative decrease of PTH levels by 50% to normal or almost normal levels [8]. Morphological picture also retains importance in the diagnostically difficult cases presenting as a relapse after surgery with curative intention. These situations are more likely to be associated with complex histology as well.

The number of immunohistochemical studies of parathyroid tissues is limited; published data are diverse and occasionally controversial, and technologies have changed over the years. To overcome these problems, we set up the current study. Here we explored a representative group (179 glands) of parathyroid pathologies, including hyperplasia, adenoma and carcinoma aiming to detect the expression of proteins that potentially could serve either as morphological diagnostic adjuncts or targets of personalised treatment. We also evaluated the molecular heterogeneity that could influence both diagnostic and scientific studies, e.g., fine needle aspiration and tissue microarray studies, respectively. The research targets included a wide spectrum of molecules that were involved in regulation of cell cycle and apoptosis, as well as tumour suppressors, intermediate filaments and adhesion factors.

Material and methods

The study quintessence, ethical principles and case selection

The study was designed as a retrospective immunohistochemical investigation of consecutive, surgically removed parathyroid tumours and tissues in a representative group. All the operations were performed with curative intent, based solely on clinical indications. The patients were not subjected to any additional procedures and/or experimental investigations. The research was carried out in accordance with the Declaration of Helsinki. The study was approved by the Committee of Ethics of Riga Stradins

University (Riga, Latvia). All the patients' data were treated confidentially and anonymously.

The consecutive cases of surgically removed parathyroid glands were identified via an archive search over a 5-year period in a single university hospital. The initial inclusion criteria comprised a verified morphological diagnosis of a parathyroid tumour or hyperplasia in a tissue material routinely submitted after clinically indicated surgical treatment. Morphologically non-altered glands were retrieved from consecutive parathyroid or thyroid surgical specimens. The clinical case histories were reviewed then, and patients with documented secondary or tertiary hyperparathyroidism or with positive family history of hyperparathyroidism were excluded from further analysis. Demographic data (age at the time of operation and gender) were retrieved from the medical documentation.

Surgical pathology evaluation

During the initial diagnostic testing, pathology data were obtained via uniform, protocol-based gross and microscopic examination of the parathyroid surgery materials. Grossly, mass lesions were characterized by the largest diameter, colour, consistency and relations with other structures, e.g., thyroid gland. Tissues were sampled widely from the capsule/border and middle of any nodule and grossly involved adjacent tissues (if applicable). The grossing was followed by routine laboratory processing. The samples were fixed in neutral buffered 10% formalin (Sigma-Aldrich/Merck, Saint Louis, USA), vacuum-processed (Tissue-Tek® VIP™ 5; Sakura Seiki Co., Ltd., Nagano and Tokyo, Japan), embedded (TES 99; Medite Medical GmbH, Burgdorf, Germany), cut (HM 360; Microm/Zeiss Group, Walldorf, Germany) in 3 μm thickness and stained (TST 44; Medite) with haematoxylin and eosin. Within the frames of current study, the slides were reviewed under light microscope (Eclipse Ci-L, Nikon, Tokyo, Japan) by two independent observers to verify the morphological diagnosis in accordance with the following criteria.

Parathyroid carcinoma was diagnosed, if there was an unequivocal evidence of any of the following features: 1) invasive growth involving the surrounding tissues as thyroid gland, soft tissues or oesophagus; 2) vascular or 3) perineural invasion; 4) presence of metastases [3, 9, 10, 11]. The surgical material was thoroughly evaluated to identify lymph nodes potentially harbouring regional metastases, and the clinical documentation was checked for the data on the presence of distant metastases.

To distinguish between the benign causes of primary hyperparathyroidism, historical morphological criteria were combined by data provided by preoperative localisation studies and the effect of gland removal on parathyroid hormone levels [12]. Parathyroid adenoma was diagnosed if a single encapsulated or demarcated, non-invasive parathyroid neoplasm lacking intralesional adipose tissue was found in a patient experiencing surgery-related decrease on the parathyroid hormone level [7, 12, 13]. Parathyroid hyperplasia was diagnosed in cases of multiglandular hyperplastic morphology showing mixture of parenchymal and fat cells with increased parenchyma-to-fat ratio [7, 13, 14]. Controversial cases were excluded from further analysis.

Immunohistochemical visualisation and assessment

Immunohistochemical visualisation (IHC) was performed on a single representative block of a parathyroid tumour or non-neoplastic gland. For IHC, 3 μm thick sections were cut by an electronic rotary microtome HM 360 (Microm) on electrostatic glass slides (Histobond, Marienfeld, Germany). After deparaffinisation, antigen retrieval was performed in a microwave oven (3 × 5 min. at 800 W) using a basic TEG (pH 9.0) buffer (DAKO, Glostrup, Denmark), followed by blocking of endogenous peroxidase (Sigma-Aldrich). The sections were incubated with primary antibodies (Table I) for 60 minutes at room temperature in the magnetic incubation tray. Bound antibodies were detected by the enzyme-conjugated polymeric visualisation system EnVision, linked with horseradish peroxidase using 3,3'-diaminobenzidine as the chromogen. All primary antibodies, secondary and ancillary IHC reagents were manufactured by DAKO except anti-parafibromin by Abcam (Cambridge, UK). Positive and negative quality control stains were invariably performed and reacted appropriately.

The expression of parafibromin was evaluated as qualitative binary estimate: complete loss of nuclear expression *versus* presence of nuclear reactivity [11]. For all other markers, the fraction of positive cells was detected by computer-assisted (NIS-Elements, Nikon) counting of cells showing appropriate expression pattern (nuclear, cytoplasmic or membranous, see Table I). Within the current study, cells were counted by standard approach, evaluating 1000 sequential tumour/parathyroid cells at high-power magnification (400×; Eclipse Ci-L, Nikon). For antigens showing heterogeneous intensity of positive reaction, the IHC reactivity was classified into four intensity levels: 0, negative; 1, low; 2, moderate and 3, high [15, 16]. The relative extent (%) was measured as the fraction of cells expressing the given marker at the given intensity level. The final IHC score was calculated as the sum of the mathematical products of the intensity and the relative extent as described by Briede *et al*., 2020 [16]. For nuclear antigens displaying heterogeneity as highly focal expression in the present study, the highest and lowest fraction

Table I. The characteristics and evaluation of immunohistochemical panel

Antigen	Antibody	Clone	Dilution	Pattern	Evaluation
Ki-67 protein	MMAH	MIB-1	1:100	Nu	F, HSF, CSF, Δ
$p21^{WAF1/Cip1}$ protein	MMAH	SX118	1:25	Nu	F, HSF, CSF, Δ
Cyclin D1	MRAH	EP12	1:500	Nu	F, HSF, CSF, Δ
p53 protein	MMAH	DO-7	1:400	Nu	F, IHC score[1]
$p27^{Kip1}$ protein	MMAH	SX53G8	1:50	Nu	F, IHC score
Bcl-2 oncoprotein	MMAH	124	1:800	Ct	F, IHC score
E-cadherin	MMAH	NCH-38	1:50	M	F, IHC score
Phagocytic glycoprotein 1 CD44	MMAH	DF1485	1:50	M	F, IHC score
CD56	MMAH	123C3	1:100	M	F, IHC score
Vimentin	MM	V9	1:200	Ct	F, IHC score
Cytokeratin 19	MMAH	RCK108	1:200	Ct	F, IHC score
Parafibromin	PR	NA	1:500	Nu	QB

[1] The IHC score was calculated as the sum of the mathematical products of the intensity and the relative extent for antigens showing heterogeneous intensity of positive reaction. The IHC reactivity was classified into four intensity levels: 0, negative; 1, low; 2, moderate and 3, high. The relative extent (%) was measured as the fraction of cells expressing the given marker at the given intensity level {16}.

CD – cluster of differentiation; MMAH – monoclonal mouse antibody against human antigen; MRAH –monoclonal rabbit antibody against human antigen; MM – monoclonal mouse antibody; PR – polyclonal rabbit antibody; NA – not applicable; Nu – nuclear; Ct – cytoplasmic; M – membranous; F – mean fraction of positive cells (per 1000 cells); HSF – the highest fraction of positive cells (per 1000 cells) in hot spots; CSF – the lowest fraction of positive cells (per 1000 cells) in cold spots; Δ – the heterogeneity measure reflecting the difference between HSF and CSF within the case; IHC – immunohistochemical; QB – qualitative binary estimate (complete loss of nuclear expression versus presence of nuclear reactivity)

was determined as the percentage of positive cells in the hot or cold spots, respectively [17]. These spots were identified by visual low-power (100×) screening of the whole slide [18]. The cell counting was performed by computer-assisted approach (NIS-Elements, Nikon) at high-power magnification (400×). The difference between highest and lowest values was calculated for each case.

Statistical analysis

The statistical analysis was performed using the IBM SPSS Statistics Version 20.0 statistical software package (International Business Machines Corp., Armonk, New York, USA). The assumption check of normality was carried out by the Shapiro-Wilk test. For descriptive statistics, mean ± standard deviation (SD), median ± interquartile range (IQR) and frequency were calculated as appropriate. In short, mean values were presented for normally distributed continuous variables while medians were reserved for other continuous variables. Categorical data were characterized by frequency. For mean values and frequencies, 95% confidence intervals (CI) were detected. Freeman-Halton extension of the Fisher's exact test was applied to contingency tables of categorical data. Kruskal-Wallis one-way analysis of variance by ranks was used to compare continuous variables. The post-hoc analysis with Bonferroni correction was performed. Any difference was considered statistically significant, if the corresponding p value was less than 0.05 [16, 18].

Results

The study group comprised 102 adenomas, 27 cases of primary parathyroid hyperplasia and 45 parathyroid glands lacking neoplastic or hyperplastic morphology. In addition, 5 parathyroid carcinomas were evaluated to illustrate the molecular trends upon malignant change. The demographic characteristics of the patients as well as gross size of the pathological glands are shown in Table II. All normal glands were identifiable only by microscopy.

The mean proliferation fraction by Ki-67 (Table III) disclosed statistically significant differences ($p < 0.001$) between the groups. The mean cellular proliferation in adenomas (1.57%; 95% CI: 1.30-1.84) and hyperplastic glands (0.98%; 95% CI: 0.71-1.25) statistically significantly exceeded the values recorded in normal parathyroid tissues (0.38%; 95% CI: 0.17-0.59) albeit the biological differences were minor. Analogous findings were obtained by the hotspot analysis, i.e., comparing the highest proliferative activities: 1.04% (95% CI: 0.63-1.45) in normal glands; 2.84% (95% CI: 2.44-3.24) in primary parathyroid hyperplasia and 3.54% (95% CI: 3.08-4.00) in adenomas. In comparison with normal and benign tissues, parathyroid carcinoma featured higher mean (5.78%; 95% CI: 0.18-11.38) and hotspot (11.76%; 95% CI: 0.66-22.86) proliferation fractions. High variability was observed in all groups underlined by the finding that the odds between the highest and lowest proliferation fraction within the same case almost equalled the highest fraction. The heteroge-

Table II. The clinical features of parathyroid glands and patients affected by parathyroid mass lesions

Parameter	Diagnosis			p value
	Parathyroid adenoma	Primary parathyroid hyperplasia	Parathyroid carcinoma	
Mean size of the affected parathyroid, cm ±SD (range)	2.7 ±1.5 (0.8-7.5)	2.4 ±1.0 (1.2-4.5)	2.7 ±0.9 (1.6-4.0)	0.265
Proportion of females, % (95% CI)	85.3 (77.0-91.0)	88.9 (71.1-97.0)	80.0 (36.0-98.0)	0.427
Mean age, years ±SD (range)	60.8 ±11.7 (34-76)	57.1 ±10.9 (45-74)	48.2 ±13.6 (35-66)	**0.029**

SD – standard deviation; CI – confidence interval

neity manifested mainly as clustering of the positive nuclei, leading to a remarkable hotspot pattern.

Regarding the nuclear expression of p21, both mean and hotspot scores showed significant differences between the studied groups (both $p < 0.001$). The highest values were observed in primary parathyroid hyperplasia both by mean assessment (15.68%; 95% CI: 13.39-17.99) and by hotspot analysis (29.83%; 95% CI: 24.29-35.37). Parathyroid adenomas yielded the next highest levels of p21 protein: mean fraction, 12.77% (95% CI: 11.35-14.19); in hot spots, 23.69% (95% CI: 21.07-26.31). In adenomas and hyperplastic glands, the mean and hotspot fraction of p21-expressing cells significantly (all $p < 0.05$) exceeded the values observed in normal glands. The up-regulation of p21 in carcinomas (mean 7.57%; 95% CI: 0.00-18.84; hotspot fraction 15.60%; 95% CI: 0.00-33.59) differed from normal tissues (mean 3.09%; 95% CI: 2.25-3.93; hotspot fraction 3.82%; 95% CI: 2.89-4.75) but did not reach the levels observed in benign parathyroid pathologies. Heterogeneity of p21 expression was brightly evident as tight foci of positive cells (Fig. 1).

Regarding the mean expression of cyclin D1, the overall differences lacked statistical significance ($p = 0.095$). Nevertheless, by CI analysis, the mean fraction of cyclin D1-positive cells in primary parathyroid hyperplasia (24.78%; 95% CI: 14.56-35.00) was significantly higher than in adenomas (12.01%; 95% CI: 10.46-13.56) or non-altered parathyroid tissues (10.11%; 95% CI: 6.82-13.40). In contrast with mean values, the analysis of both hot and cold spots disclosed significant differences of cyclin D1 expression between all groups ($p = 0.002$ and $p = 0.006$, respectively). Primary parathyroid hyperplasia and carcinoma were characterised by high expression of cyclin D1 while adenomas showed modestly increased levels (Table III). Adenomas also possessed marked heterogeneity. Interestingly, the cold spots in adenomas were characterised by even lower fraction of p21-expressing cells than observed in normal tissues: 3.41% (95% CI: 2.52-4.30) in adenomas *versus* 8.75% (95% CI: 5.48-11.47) in unaltered parathyroid glands. The dominant pattern of cyclin D1 heterogeneity was the clustering of the positive cells in hot spots.

All investigated types of parathyroid tissues were almost devoid of p53 protein as detected by immunohistochemistry (Table IV). Significant differences were identified regarding p27 score ($p = 0.005$) and fraction of p27-positive cells ($p = 0.010$), implicating loss of p27 in parathyroid carcinoma. The mean fraction of p27-positive cells in parathyroid carcinoma was only 59.00% (95% CI: 13.29-100.00), contrasting with normal glands (97.86%; 95% CI: 96.12-99.60); primary parathyroid hyperplasia (94.33%; 95% CI: 90.87-97.79) and adenoma (92.82%; 95% CI: 89.68-95.96). Considering p53 and p27 proteins, the heterogeneity was not pronounced which was partially attributable to extremes of reactivity manifesting as almost complete absence of target or nearly diffuse positive expression (Fig. 1), respectively. Variability of staining intensity was the leading manifestation of heterogeneity. To account for this, the mean IHC score was detected; it confirmed the same findings as highlighted by the mean fraction of positive cells.

There was a trend to down-regulation of Bcl-2 protein in parathyroid carcinoma although the findings lacked overall statistical significance ($p = 0.449$). In normal glands, Bcl-2 expression was observed in 75.63% of cells (95% CI: 64.70-86.56), contrasting with only 28.22% in carcinomas (95% CI: 0.00-76.38). Parathyroid adenomas and hyperplastic tissues were characterised by intermediate values: 66.68% (95% CI: 59.71-73.65) and 61.25% (95% CI: 44.28-78.22), respectively. Variability of staining intensity was the leading manifestation of heterogeneity. To account for this, the mean IHC score was applied; it highlighted the same trends as the mean fraction of positive cells.

Regarding cell adhesion molecules (Table V), a trend to down-regulation of E-cadherin was found in all proliferative mass lesions, contrasting with more intense membranous expression in normal parathyroid glands (Fig. 1). The mean final IHC score in normal tissues was 2.25 (95% CI: 2.05-2.45). In contrast, hyperplastic glands showed down-

Table III. Proliferation activity and cell cycle regulation in parathyroid tissues and tumours

Marker	Adenoma	Primary hyperplasia	Carcinoma	Normal glands	p value
Ki-67					
Lowest F*, % ±SD (range)	0.19 ±0.53 (0.00-2.75)	0.00 ±0.00 (0.00-0.00)	0.00 ±0.00 (0.00-0.00)	0.00 ±0.00 (0.00-0.00)	0.253
95% CI	0.09-0.29	0.00-0.00	0.00-0.00	0.00-0.00	NA
Mean F, % ±SD (range)	1.57 ±1.38 (0.34-6.76)	0.98 ±0.69 (0.35-2.26)	5.78 ±4.51 (1.27-13.33)	0.38 ±0.71 (0.00-2.75)	**< 0.001**
95% CI	1.30-1.84	0.71-1.25	0.18-11.38	0.17-0.59	NA
Highest F**, % ±SD (range)	3.54 ±2.33 (0.81-10.39)	2.84 ±1.02 (1.41-4.52)	11.76 ±8.94 (2.53-26.67)	1.04 ±1.38 (0.00-5.49)	**< 0.001**
95% CI	3.08-4.00	2.44-3.24	0.66-22.86	0.63-1.45	NA
Δ, % ±SD (range)	3.35 ±1.97 (0.81-9.30)	2.84 ±1.02 (1.41-4.52)	11.76 ±8.94 (2.53-26.67)	1.04 ±1.38 (0.00-5.49)	NA
p21					
Lowest F*, % ±SD (range)	2.40 ±2.98 (0.00-14.29)	2.49 ±2.11 (0.00-6.17)	1.46 ±2.79 (0.00-6.40)	2.30 ±2.69 (0.00-8.26)	0.432
95% CI	1.81-2.99	1.66-3.32	0.00-4.92	1.49-3.11	NA
Mean F, % ±SD (range)	12.77 ±7.21 (2.09-40.60)	15.68 ±5.82 (4.53-22.61)	7.57 ±9.08 (0.25-22.62)	3.09 ±2.79 (0.23-9.87)	**< 0.001**
95% CI	11.35-14.19	13.39-17.99	0.00-18.84	2.25-3.93	NA
Highest F**, % ±SD (range)	23.69 ±13.36 (3.47-63.89)	29.83 ±14.00 (10.70-55.91)	15.60 ±14.49 (0.50-38.56)	3.82 ±3.11 (0.45-11.21)	**< 0.001**
95% CI	21.07-26.31	24.29-35.37	0.00-33.59	2.89-4.75	NA
Δ, % ± SD (range)	21.29 ±13.11 (2.51-63.21)	27.34 ±14.20 (9.32-54.70)	14.13 ±11.94 (0.50-32.16)	1.52 ±1.82 (0.00-5.85)	NA
Cyclin D1					
Lowest F*, % ±SD (range)	3.41 ±4.51 (0.00-17.72)	12.20 ±19.28 (0.00-54.79)	21.78 ±43.79 (0.00-100.00)	8.75 ±10.87 (0.00-35.29)	**0.006**
95% CI	2.52-4.30	4.57-19.83	0.00-76.15	5.48-11.47	NA
Mean F, % ±SD (range)	12.01 ±7.88 (0.00-28.41)	24.78 ±25.84 (5.02-79.52)	31.49 ±39.17 (2.71-100.00)	10.11 ±10.96 (0.76-35.29)	0.095
95% CI	10.46-13.56	14.56-35.00	0.00-80.13	6.82-13.40	NA
Highest F**, % ±SD (range)	22.83 ±16.31 (0.00-62.22)	42.48 ±30.64 (7.50-98.92)	41.77 ±34.83 (13.56-100.00)	11.91 ±11.29 (0.76-35.29)	**0.002**
95% CI	19.63-26.03	30.36-54.60	0.00-85.02	8.52-15.30	NA
Δ, % ±SD (range)	19.42 ±16.52 (0.00-59.33)	30.28 ±19.57 (4.62-54.76)	20.00 ±16.50 (0.00-40.19)	3.16 ±4.06 (0.00-10.56)	NA

* *The lowest fraction of positive cells (per 1000 cells) in cold spots*

** *The highest fraction of positive cells (per 1000 cells) in hot spots*

F – fraction of positive cells; SD – standard deviation; CI – confidence interval; Δ – the difference between the highest and lowest value; NA – not applicable

regulation to 0.96 (95% CI: 0.60-1.32); adenoma yielded the score of 1.00 (95% CI: 0.86-1.14) and carcinoma – 1.27 (95% CI: 0.79-1.75). Parathyroid tissues were generally negative for CD44 except for few adenomas showing low scores. The expression of CD56 in the glandular tissues also was not significant although few tumours presented with low scores. Reactivity of CD56 in perivascular nerve fibres was found in most cases, namely, in 86/102 (84.31%; 95% CI: 75.92-90.21) adenomas, 22/27 (81.48%; 95% CI: 62.84-92.28) hyperplastic and 28/45 (62.22%; 95% CI: 47.60-74.92) normal glands as well as 2/5 (40.00%; 95% CI: 11.60-77.09) carcinomas.

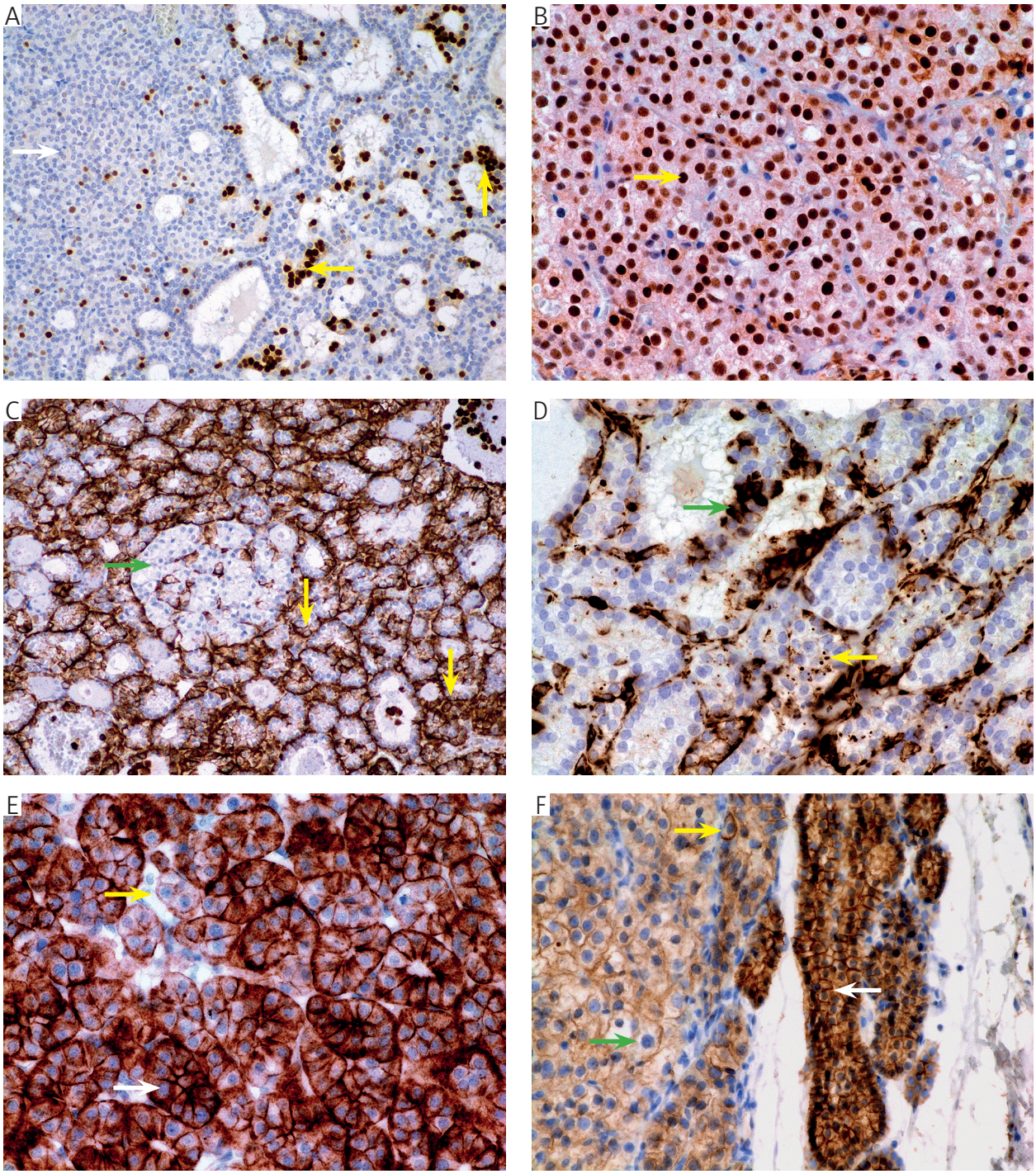

Fig. 1. Immunophenotype of parathyroid adenoma. A) Nuclear expression of p21 protein: an overview. Immunoperoxidase (IP); anti-p21WAF1/Cip1 protein, clone SX118; original magnification (OM) 100×. Note the crisp nuclear stain, marked heterogeneity manifesting as extremely dense clusters of positive nuclei (arrowheads) and negative cold foci (arrow). B) Widespread homogeneous nuclear expression of p27 protein (arrow). IP; anti-p27Kip1 protein, clone SX53G8; OM 200×. C) Expression of vimentin: an overview of nodular pattern. Note the remarkable heterogeneity, cytoplasmic reactivity in the epithelial cells (arrowheads) and the rounded negative nodule (arrow). IP; anti-vimentin, clone V9; OM 100×. D) Combined pattern of vimentin expression. Note the cytoplasmic (arrow) and perinuclear (arrowhead) reactivity in the epithelial cells. Positive mesenchymal stromal cells are visible and act as an internal control. IP; anti-vimentin, clone V9; OM 200×. E) Cytoplasmic expression of cytokeratin 19. Note the heterogeneous staining with high (arrow) and low (arrowhead)-intensity areas. IP; anti-cytokeratin 19, clone RCK108; OM 200×. F) Expression of E-cadherin. Note the high intensity in the normal gland adjacent to the adenoma (white arrow), down-regulation of E-cadherin in adenoma (green arrow) and heterogeneity underlined by intense expression in a single cell of adenoma (arrowhead). IP; anti-E-cadherin, clone NCH-38; OM 200×

Table IV. Selected tumour suppressor- and apoptosis-related proteins in parathyroid tissues and tumours

Marker	Adenoma	Primary hyperplasia	Carcinoma	Normal glands	p value
Parafibromin					
N (%)	102/ 102 (100.00)	26/ 27 (96.30)	0/5 (0.00)	45/45 (100.00)	< 0.001
95% CI	95.64-100.00	80.20-100.00	0.00-48.91	90.62-100.00	NA
p53					
Mean IHC score ±SD (range)	0.02 ±0.04 (0.00-0.14)	0.04 ±0.07 (0.00-0.20)	0.00 ±0.00 (0.00-0.00)	0.00 ±0.00 (0.00-0.00)	< 0.001
95% CI	0.01-0.03	0.01-0.06	0.00-0.00	0.00-0.00	NA
F, % ±SD (range)	0.92 ±1.84 (0.00-7.00)	2.06 ±3.61 (0.10-11.00)	0.08 ±0.04 (0.00-0.10)	0.02 ±0.04 (0.00-0.10)	< 0.001
95% CI	0.56-1.28	0.63-3.49	0.03-0.13	0.01-0.03	NA
p27					
Mean IHC score ±SD (range)	2.77 ±0.48 (0.30-3.00)	2.79 ±0.36 (2.00-3.00)	1.77 ±1.10 (0.60-3.00)	2.94 ±0.17 (2.40-3.00)	0.005
95% CI	2.68-2.86	2.65-2.93	0.40-3.00	2.89-2.99	NA
F, % ±SD (range)	92.82 ±16.00 (10.00-100.00)	94.33 ±8.75 (80.00-100.00)	59.00 ±36.81 (20.00-100.00)	97.86 ±5.79 (80.00-100.00)	0.010
95% CI	89.68-95.96	90.87-97.79	13.29-100.00	96.12-99.60	NA
Bcl-2					
Mean IHC score ±SD (range)	1.49 ±0.94 (0.00-3.00)	1.44 ±0.97 (0.00-2.00)	0.48 ±0.65 (0.00-1.20)	1.64 ±0.93 (0.10-3.00)	0.706
95% CI	1.31-1.67	1.06-1.82	0.00-1.29	1.36-1.92	NA
F, % ±SD (range)	66.68 ±35.50 (0.00-100.00)	61.25 ±42.89 (0.00-100.00)	28.22 ±38.79 (0.00-80.00)	75.63 ±36.39 (5.00-100.0)	0.449
95% CI	59.71-73.65	44.28-78.22	0.00-76.38	64.70-86.56	NA

N – number of cases; CI – confidence interval; IHC – immunohistochemical; SD – standard deviation; F – fraction of positive cells; NA – not applicable

The expression of intermediate filaments is characterised in Table VI. Statistically significant up-regulation of cytokeratin 19 ($p = 0.012$) and insignificant ($p = 0.091$) trend to more extensive expression of vimentin was observed in the proliferative parathyroid lesions. The most marked changes were evident in carcinoma. Thus, the fraction of vimentin-expressing cells increased from 9.33% (95% CI: 5.61-13.05) cells in normal tissues to 11.67% (95% CI: 6.51-16.83) in primary parathyroid hyperplasia, 19.30% (95% CI: 13.27-25.33) in adenomas and 36.80% (95% CI: 0.00-79.44) in carcinoma. Interestingly, the patterns of vimentin expression also varied (Fig. 1). Perinuclear reactivity was the only pattern in normal glands. Cytoplasmic expression was invariable in carcinomas. Hyperplastic glands and adenomas showed combination of both patterns, with tendency to more frequent cytoplasmic expression in adenomas and predominantly perinuclear pattern in primary parathyroid hyperplasia. Heterogeneity was remarkable in all groups, but only adenomas and hyperplastic glands showed nodularity of vimentin expression.

Considering cytokeratin 19 (Fig. 1), its mean final score raised from 0.26 (95% CI: 0.19-0.33) in normal glands to 0.82 (95% CI: 0.45-1.19) in primary parathyroid hyperplasia and 0.84 (95% CI: 0.68-1.01) in adenomas. In carcinoma, it was even higher: 1.02 (95% CI: 0.00-2.70). The changes featured statistical significance ($p = 0.012$).

Loss of parafibromin was invariable in all carcinomas (expression rate 0/5; 0%; 95% CI: 0.00-48.91). It was also observed in a hyperplastic gland from a single patient (1/27; 3.70%; 95% CI: 0.00-19.80). Expression of parafibromin was retained in 102/ 102 (100%; 95% CI: 95.64-100.00) adenomas, 26/27 (96.30%; 95% CI: 80.20-100.00) cases of primary hyperplasia and 45/45 (100%; 95% CI: 90.62-100.00) parathyroid glands lacking neoplastic or hyperplastic changes. The differences were statistically significant ($p < 0.001$).

Discussion

Although parathyroid surgery is becoming increasingly frequent, the differential diagnosis between

Table V. Cell adhesion molecules in parathyroid tissues and tumours

Marker	Adenoma	Primary hyperplasia	Carcinoma	Normal glands	p value
E-cadherin					
Mean IHC score ±SD (range)	1.00 ±0.71 (0.00-2.50)	0.96 ±0.92 (0.12-3.00)	1.27 ±0.39 (0.90-1.70)	2.25 ±0.67 (1.00-3.00)	0.753
95% CI	0.86-1.14	0.60-1.32	0.79-1.75	2.05-2.45	NA
F, % ±SD (range)	32.29 ±37.26 (0.00-100.00)	25.44 ±30.03 (4.00-100.00)	36.00 ±26.08 (20.00-80.00)	72.78 ±38.50 (0.00-100.00)	0.758
95% CI	24.97-39.61	13.56-37.32	3.62-68.38	61.21-84.35	NA
CD44					
Mean IHC score ±SD (range)	0.05 ±0.11 (0.00-0.38)	0.00 ±0.00 (0.00-0.00)	0.00 ±0.00 (0.00-0.00)	0.00 ±0.00 (0.00-0.00)	0.253
95% CI	0.03-0.07	0.00-0.00	0.00-0.00	0.00-0.00	NA
F, % ±SD (range)	1.79 ±4.05 (0.00-15.00)	0.00 ±0.00 (0.00-0.00)	0.00 ±0.00 (0.00-0.00)	0.00 ±0.00 (0.00-0.00)	0.159
95% CI	0.99-2.59	0.00-0.00	0.00-0.00	0.00-0.00	NA
CD56					
Mean IHC score ±SD (range)	0.04 ±0.14 (0-0.6)	0.00 ±0.00 (0.00-0.00)	0.07 ±0.09 (0.00-0.21)	0.00 ±0.00 (0.00-0.00)	0.115
95% CI	0.01-0.07	0.00-0.00	0.00-0.18	0.00-0.00	NA
F, % ±SD (range)	1.37 ±4.66 (0.00-20.00)	0.00 ±0.00 (0.00-0.00)	3.00 ±3.08 (0.00-7.00)	0.00 ±0.00 (0.00-0.00)	0.113
95% CI	0.45-2.29	0.00-0.00	0.00-6.82	0.00-0.00	NA

IHC – immunohistochemical; SD – standard deviation; CI – confidence interval; F – fraction of positive cells; CD – cluster of differentiation; NA – not applicable.

parathyroid mass lesions themselves or with other neck pathologies can still be challenging for pathologists, at least partially – because of insufficient awareness of parathyroid morphology and immunophenotype. In addition, there are quite few large-scale immunohistochemical studies exploring wide spectrum of proteins. To fill the gap, we studied 179 consecutive surgically removed parathyroid glands in order to evaluate the proteins that potentially could serve either as morphological diagnostic adjuncts or targets of personalised treatment. To the best of our knowledge, this is the first study systematically evaluating IHC heterogeneity in parathyroid glands. Significant heterogeneity was observed as hotspot pattern (Ki-67, p21, cyclin D1), intensity variation (p53, p27, Bcl-2) and changes in expression pattern (vimentin).

Parafibromin. Parafibromin is the protein coded by *Cell Division Cycle 73* (*CDC73*) gene known also as *HRPT2* (*hyperparathyroidism 2*). In 2002, germline mutation of *CDC73* was found in families affected by the autosomal dominant hyperparathyroidism-jaw tumour syndrome that was associated with increased lifetime risk of parathyroid carcinoma approaching 15% in mutation carriers. Indeed, in the hyperparathyroidism-jaw tumour syndrome patients, carcinoma is responsible for 15-37.5% of hyperparathyroidism cases. Later, somatic *CDC73* mutations were found in sporadic tumours. Currently, it is thought that 77% of parathyroid carcinomas and less than 1% of parathyroid adenomas harbour *CDC73* mutation [11].

As *CDC73* mutation testing is not widely available, loss of nuclear expression of parafibromin by immunohistochemistry has been accepted as a surrogate test [11, 19, 20, 21]. Parafibromin is a tumour suppressor protein that induces cell cycle arrest by repressing cyclin D1 [22]. It is involved in the regulation of p53 pathway [11]. The name of it, parafibromin, reflects the association with parathyroid pathologies and ossifying fibromas of maxillary and mandibular bones within the hyperparathyroidism-jaw tumour syndrome [11, 12]. Since the first discoveries, absence of parafibromin has been associated with diagnostic evidence [23] and worse prognosis of parathyroid carcinomas [21] and malignant behaviour of tumours histologically diagnosed as atypical adenomas [24]. However, controversies exist that can be at least in part attributed to technological differences and challenges [11], nuclear, nucleolar or cytoplasmic location of reactivity [9, 25, 26] or cases showing partial or weak expression [9, 11, 27, 28].

Loss of parafibromin has been reported in 60-100% of parathyroid carcinomas [19, 20, 29] and 4.5-18%

Table VI. Intermediate filaments in parathyroid tissues and tumours

Marker	Adenoma	Primary hyperplasia	Carcinoma	Normal glands	p value
Vimentin					
Mean IHC score ±SD (range)	0.57 ±0.91 (0.00-2.70)	0.35 ±0.39 (0.00-1.20)	1.08 ±1.05 (0.04-2.70)	0.28 ±0.37 (0.00-1.20)	0.105
95% CI	0.39-0.75	0.20-0.50	0.00-2.38	0.17-0.39	NA
F, % ±SD (range)	19.30 ±30.69 (0.00-90.00)	11.67 ±13.05 (0.00-40.00)	36.80 ±34.34 (2.00-90.00)	9.33 ±12.37 (0.00-40.00)	0.091
95% CI	13.27-25.33	6.51-16.83	0.00-79.44	5.61-13.05	NA
Heterogeneity, N (%)	56/102 (54.90)	19/27 (70.37)	5/5 (100.00)	15/45 (33.33)	0.002
95% CI	45.24-64.21	51.35-84.32	51.09-100.00	21.30-47.99	NA
Nodularity, N (%)	13/102 (12.75)	4/27 (14.81)	0/5 (0.00)	0/45 (0.00)	0.06
95% CI	7.47-20.73	5.30-33.10	0.00-48.91	0.00-9.38	NA
Cytoplasmic expression, N (%)	48/57 (84.21)	9/21 (42.86)	5/5 (100.00)	0/21 (0.00)	**< 0.001**
95% CI	72.41-91.69	24.44-63.48	51.09-100.00	0.00-18.24	NA
Perinuclear expression, N (%)	27/57 (47.37)	18/21 (85.71)	2/5 (40.00)	21/21 (100.00)	**< 0.001**
95% CI	34.99-60.08	64.52-95.86	11.60-77.09	81.76-100.00	NA
Cytokeratin 19					
Mean IHC score ±SD (range)	0.84 ±0.84 (0.00-2.50)	0.82 ±0.93 (0.02-2.50)	1.02 ±1.35 (0.00-2.85)	0.26 ±0.23 (0.00-0.80)	**0.012**
95% CI	0.68-1.01	0.45-1.19	0.00-2.70	0.19-0.33	NA
F, % ±SD (range)	35.83 ±34.46 (0.00-100.00)	32.83 ±37.14 (1.00-100.00)	34.22 ±44.99 (0.10-95.00)	12.60 ±11.21 (0.00-40.00)	0.748
95% CI	29.06-42.60	18.14-47.52	0.00-90.08	9.23-15.97	NA
Heterogeneity, N (%)	62/102 (60.78)	24/27 (88.89)	5/5 (100.00)	30/45 (66.67)	**0.017**
95% CI	51.08-69.71	71.12-96.97	51.09-100.00	52.01-78.70	NA
Nodularity, N (%)	15/102 (14.71)	14/27 (51.85)	0/5 (0.00)	15/45 (33.33)	**0.0002**
95% CI	9.00-22.97	33.98-69.26	0.00-48.91	21.30-47.99	NA

IHC – immunohistochemical; SD – standard deviation; CI – confidence interval; F – fraction of positive cells; N – number of cases; NA – not applicable

of adenomas [19, 20, 29, 30]. In some cohorts, all adenomas have been positive [27, 31]. In our study, we succeeded to show invariable lack of parafibromin in carcinomas and nuclear expression – in adenomas. In addition, all normal parathyroid tissues were positive in accordance with Wang *et al*., 2012 [29].

Although parafibromin positivity was expected in parathyroid hyperplasia [29, 31], we experienced a single negative case. Despite the negative family history, the hyperparathyroidism-jaw tumour syndrome could not be completely excluded in this single case as the patient was lost from follow-up at the time of this study. Hyperparathyroidism-jaw tumour syndrome can present as seemingly sporadic parathyroid lesion. It has been estimated that 20% of apparently sporadic parathyroid carcinomas in fact are associated with germline *CDC73* mutation [11, 12]. Further, genetically confirmed hyperparathyroidism-jaw tumour syndrome can present with multiglandular parathyroid hyperplasia [32] although single or multiple [12, 30] parathyroid adenomas or parathyroid carcinomas are the classic features of this syndrome (90% of cases), along with benign fibro-osseous lesions of jaw bones (30%). In addition, renal cysts are present in 10% of cases and uterine leiomyomas in 40% of female patients [12, 32].

Although immunohistochemistry for parafibromin is technically demanding and the results show overlap between adenoma and carcinoma, gene assessment also yields overlapping data. Thus, mutations of *CDC73*/*HRPT2* have been reported in only 60-90.9% of parathyroid carcinoma and 4.5-6% of adenomas [19, 20, 30]. In our experience, albeit the immunohistochemical stain is technically challenging, it has a rewardingly high diagnostic value. The procedure must be followed rigorously, and repeated stains can be necessary, but reliable final

result with appropriate internal positive controls can be reached.

Ki-67. Ki-67 is a nuclear protein that is expressed during the active phase of cell cycle while strongly down-regulated during the G_0 phase. Thus, the presence of immunohistochemically detectable Ki-67 identifies proliferating cells. Due to this feature, IHC for Ki-67 has become an important part of manifold morphological protocols in tumour diagnostics, including grading, molecular classification, prognostic evaluation and prediction of treatment efficacy. Despite the well-known clinical value, the molecular biology of Ki-67 protein has been studied in depth only recently. Currently, mitotic, regulatory and the interphase functions of Ki-67 are identified. During mitosis, Ki-67 participates in the build-up of perichromosomal layer: a ribonucleoprotein sheath that coats the condensed chromosomes and prevents them from aggregation. Unlike several other proteins, Ki-67 is a mandatory component for the development of perichromosomal layer. In addition, Ki-67 participates in cell cycle regulation; these mechanisms involve interaction with p21 protein pathways. During interphase, Ki-67 protein maintains the structure of heterochromatin [33, 34, 35].

Increased cellular proliferation has been shown in parathyroid tumours and hyperplasia in contrast to non-altered glands [36]. More recently, statistically significantly higher proliferation activity was observed in parathyroid carcinomas than in adenomas [37]. The reported mean proliferation fraction in carcinoma ranges from 6% [38] to 8.4% [39] or even 13.9% [40]. In adenomas, the mean proliferation index by Ki-67 is reported as 1.9 [41] – 4.26% [42] significantly exceeding the Ki-67 levels in residual parathyroid tissues [43]. However, controversies exist. Thus, Kaczmarek *et al*. reported that normal and hyperplastic tissues were characterised by proliferation fractions of 3.5% and 1.8%, respectively [41].

In our study, we confirmed significant differences in Ki-67 expression. Both by mean and the highest values, the proliferative activity increased from normal to hyperplastic glands, adenoma and carcinoma. We also observed significant heterogeneity with a prominent hotspot pattern. The presence of tissue heterogeneity can cause methodologic discrepancies, e.g., in studies using tissue microarrays – a classic method in pathology that allows simultaneous testing of large material for numerous markers by combining tissue cores from multiple cases into a single slide [44, 45]. Microarrays have also been used in parathyroid research [46]. Despite the said benefits, microarrays are vulnerable by the selection of the region of interest, which may or may not include hot or cold spots. We showed in the current study that the same statistically significant differences could be found analysing the mean ($p < 0.001$) or the highest ($p < 0.001$) proliferation fraction leading to the same conclusions, but this was not relevant to cold spots. Thus, heterogeneity can indeed influence the results and conclusions obtained via microarrays or similar techniques. In addition, the approach to Ki-67 counting will have utmost significance deciding on the diagnostic criteria of carcinoma, namely, the cut-off level. Besides the impact on cohort-based scientific data and diagnostic thresholds, heterogeneity can affect the measurement obtained in a particular patient, e.g., via fine needle aspiration. The heterogeneity should be acknowledged in future studies by routine use of relevant parameters to characterise it.

Cyclin D1. The cyclin D1 is known as an important molecular switch in the proliferation control as well as a transcriptional regulator. As an allosteric activator, it forms a complex with cyclin dependent kinases 4 and 6 (CDK4 and CDK6) that phosphorylate and thus inactivate the tumour suppressor protein Rb, resulting in the cell cycle progress from the G_1 to S phase [47, 48]. The overexpression of cyclin D1 in parathyroid tumours can be attributable to pericentric inversion of chromosome 11p that results in *CCND1* gene control by parathyroid hormone gene promoter. However, this inversion is seen in lower frequency than the overexpression of the relevant cyclin D1 protein, e.g., 5-8% *versus* 40% in adenomas. Thus, other mechanisms are acting including gene amplification, other rearrangements, transcriptional activation [47] or deranged degradation [49].

In transgenic mice, overexpression of the cyclin D1-coding gene resulted in hyperparathyroidism. This finding was consistent with the primary role of cyclin D1 in parathyroid hyperfunction. Morphologically, the animals developed hyperplasia as well as asymmetrical encapsulated nodular growths bearing tubular architecture and compressing adjacent gland, thus closely resembling adenomas. By IHC, no cyclin D1 expression was found in parathyroid tissues of wild-type animals while irregular positive staining was found in hyperplastic glands of transgenic mice [50]. Similarly, we found significant up-regulation of cyclin D1 in hyperplastic glands featuring remarkable heterogeneity of hotspot pattern. Notably, the highest fraction of cyclin D1-positive cells in hyperplasia was significantly higher as in adenoma hypothetically showing the cyclin D1 as an early molecular driver in parathyroid cell proliferation. Other molecular mechanisms are necessary for neoplastic changes, e.g., escape from apoptosis or loss of parafibromin-related counterbalance of cyclin D1.

Interestingly, in the current study, the fraction of cyclin D1-expressing cells was statistically significantly different between PPH and adenomas. The differences were also notable from the biological point of view, contrasting with minor margin regarding Ki-67. Hypothetically, cyclin D1 could be

useful in the differential diagnosis between adenomas and PPH, with high levels preferring a hyperplastic process. This assumption is in accordance with the pathogenetic importance of cyclin D1 in the early steps of parathyroid pathology. However, considering the general key role of cyclin D1 in parathyroid diseases, additional studies would be necessary. Correlations between cyclin D1 expression and surgical cure *versus* recurrence should also be evaluated.

Intertumoural heterogeneity of cyclin D1 has been noted before, both in adenomas and carcinomas [19, 20]. We observed both significant intertumoural heterogeneity along with remarkable intralesional heterogeneity with presence of cold and hot spots.

Several research groups have evaluated IHC expression of cyclin D1 in parathyroid carcinoma. Truran *et al*. observed cyclin D1 in a minor fraction of parathyroid carcinoma cases (8.3%) and therefore disregarded to include it in the diagnostic panel of this malignancy [23]. By Stojadinovic *et al*., nuclear expression of cyclin D1 (by cut-off 5%) was found in 9% of adenoma and 18% of carcinoma; the difference lacked statistical significance [46]. Similarly, Rodriguez *et al*. concluded that overexpression of cyclin D1 could not be used to reliably differentiate between adenoma and carcinoma [51]. In our experience, the set-up of scoring protocols (mean *versus* highest fraction of cyclin D1-positive cells) can influence the degree of statistical significance and thus lead to different conclusions.

Although higher levels of wild-type parafibromin have been shown to block expression of cyclin D1 [52], by IHC, no correlation has been reported by cyclin D1 and parafibromin expression in parathyroid pathology [19, 20, 53]. Thus, these molecular events are neither related nor mutually exclusive but can be sequential or additive. In our study, loss of parafibromin was almost completely limited to parathyroid carcinoma and thus could not explain the variable degree of cyclin D1 overexpression in parathyroid hyperplasia and adenoma. Nevertheless, it can suggest functionality of high cyclin D1 levels in parafibromin-negative carcinoma in contrast with equally high levels of cyclin D1 in benign proliferative lesions harbouring wild-type parafibromin.

p27. The p27 is a cyclin-dependent kinase inhibitor and tumour suppressor that inhibits cell cycle progression, mediating G_1 arrest. Malignant cells can lose p27 expression due to impaired synthesis or accelerated degradation, or inappropriate intracellular localisation of the relevant protein [54, 55].

In the present study, we found statistically significant differences ($p = 0.010$) between the explored groups suggesting loss of p27 upon malignant change. In normal parathyroid glands, practically all cells (97.86%; 95% CI: 96.12-99.60) expressed p27 protein. The nuclear expression was almost completely retained in primary parathyroid hyperplasia (94.33%; 95% CI: 90.87-97.79) and adenoma (92.82%; 95% CI: 89.68-95.96) while the levels were remarkably lower in parathyroid carcinoma (59.00%; 95% CI: 13.29-100.00). Decreasing levels of p27 expression have been reported in normal parathyroid glands, hyperplastic tissues, parathyroid adenoma and carcinoma, namely, 89.6%, 69.6%, 56.8% and 13.9%. Initially, lack of differences in mRNA levels was thought to indicate posttranslational events [39]. Subsequently, decreased p27 mRNA expression was demonstrated in adenoma, compared to normal gland [56]. However, the regulation of p27 activity is complex. It involves modulation of transcription, effects of p27 transcript-targeting microRNAs and manifold reactions at the protein level. Different mechanisms degrade p27 protein in nuclear and cytosolic compartments, and nucleocytoplasmic shuttling ensures additional regulatory properties. Suppression of p27 in carcinoma was verified by Arvai *et al*., 2012 [57], and the difference between adenomas and carcinomas (80% of adenomas *versus* 18% of carcinomas by cut-off 30%) was found to be statistically significant [46]. Nevertheless, contradictory findings have been reported, e.g., Fernandez-Ranvier *et al*. observed that p27 expression did not differ between parathyroid tumours [31]. Our data indicate loss of p27 protein expression along with malignant course but no significant differences between normal, hyperplastic or adenomatous parathyroid tissues.

p21. The p21 protein controls cell cycle progression, apoptosis and transcription. It is the key mediator of cell cycle arrest in response to DNA damage [58] and a component of p53 pathway [46]. The expression of p21 can have dual effects, including suppression or enhancement of apoptosis [58, 59].

In the present study, we observed significant differences regarding the mean ($p < 0.001$) and highest ($p < 0.001$) values of p21 protein expression in normal parathyroid tissues, hyperplasia, adenoma and carcinoma. Normal glands were characterised by the lowest levels of expression (mean fraction, 3.09%; hotspot fraction, 3.82% of parenchymal cells) while the most extensive expression was seen in hyperplasia (15.68% and 29.83%, respectively) and adenoma (12.77% and 23.69%). Parathyroid carcinoma demonstrated intermediate values (7.57% and 15.60%). These findings indirectly indicate either the duality of p21 [59] or a protective action that is up-regulated in hyperplastic and benign proliferations but lost upon malignant change.

Our data support and expand the previous reports. Thus, in tissue microarrays, nuclear expression of p21 (by cut-off at the level of 10%) was found in 58% of adenoma and 55% of carcinoma [46]. The remarkable heterogeneity that was observed in the current study hinted on cautious interpretation

of results obtained by microarrays. However, the differences and trends in p21 expression were preserved both in mean *versus* hotspot counting modes. Further research is necessary, accounting for the high heterogeneity, especially if changing p21 expression levels by means of gene editing will be considered as an additive therapy for specific cancers to suppress tumorigenesis phenotypes or to reduce drug resistance [59].

Bcl-2. Bcl-2 protein is known for its anti-apoptotic function [60]. Immunohistochemical studies of apoptosis by monoclonal antibody against single-stranded DNA have showed statistically significant ($p = 0.034$) reduction of apoptosis in primary parathyroid hyperplasia contrasting with parathyroid tumours [36]. Previously, widespread (at least 80% of cells) cytoplasmic Bcl-2 expression has been reported in all normal parathyroid glands contrasting with invariable negativity in three cases of carcinomas [61]. Suppression of Bcl-2 in carcinoma has been confirmed in more recent studies [57]. By cut-off level at 50% of cells, Bcl-2 expression was found in 98% of adenoma and 55% of carcinoma cases [46]. Our findings indicated corresponding trends, namely, down-regulation of Bcl-2 in parathyroid carcinomas: while 75.63% (95% CI: 64.70-86.56) of normal parathyroid cells expressed Bcl-2, the fraction in carcinomas was as low as 28.22% (95% CI: 0.00-76.38). By IHC score, accounting for the heterogeneity of expression intensity, normal tissues yielded the value of 1.64 (96% CI: 1.36-1.92) while carcinoma scored as 0.48 (95% CI: 0.00-1.29).

Regarding benign parathyroid lesions, controversial data have been reported. In different studies, Bcl-2 expression in adenomas ranged from 55% to 73% and even 98% [43, 46, 61]. Despite the previously noted reduction of apoptosis in hyperplastic parathyroid glands [36], lower expression of Bcl-2 in hyperplasia than in normal glands and adenomas has been reported as well suggesting other regulatory mechanisms [41]. Notably, the differences were remarkable: the mean area fraction was 0.172 per 1 mm^2 in hyperplasia, contrasting with 0.643 in adenomas and 0.648 in control tissues [41]. Other authors have found up-regulation of Bcl-2 in benign tumours noting that 73% of adenomas and 31% residual rims of parathyroid tissues were positive [43]. Our data suggest almost equal levels of Bcl-2 expression in adenomas, hyperplastic and non-altered glands.

p53. The "genome guard", p53 protein is normally found within cells in small quantities due to a short half-life. *TP53* mutations can result in the synthesis of aberrant p53 proteins that have longer half-lives and therefore accumulate in cells reaching such intracellular concentration levels that can be detected by immunohistochemistry. The *TP53* mutation analyses and p53 IHC provide two different levels of molecular examination lacking unequivocal correlation between gene mutations and aberrant p53 protein expression [62].

Regarding p53 in parathyroid tumours, facilitated degradation of the relevant mRNA might be implicated. Parafibromin, the protein product of *CDC73*/*HRPT* gene, can specifically bind to mature messenger RNA of p53 resulting in mRNA destabilisation [26]. Enhanced association with mutant parafibromin would result in facilitated degradation of p53 mRNA. The final outcome would be absence of p53 expression by immunohistochemistry and enhanced cellular proliferation in parathyroid carcinoma while benign lesions retained wild-type protein. The general landscape of p53 expression in parathyroid diseases thus would lack diagnostic differences. Indeed, invariable negative p53 expression in normal parathyroid as well as benign and malignant tumours has been reported previously [46, 61]. However, other research teams have identified reactivity in even 15% of adenoma cases [43] and overexpression of p53 in carcinoma [57].

In our study, the levels of p53 expression were low. Both normal glands and carcinomas were almost completely devoid of p53 reactivity. Modest up-regulation was observed in few cells of adenoma (0.92%) and primary parathyroid hyperplasia (2.06%). Considering the low intensity of staining, this finding can be attributable to the ability of DAKO primary antibody, clone DO-7, to react with wild-type p53 protein. In carcinomas, showing invariable loss of nuclear parafibromin, the expression of p53 protein was negligibly low. Despite the observed statistically significant difference between groups, p53 protein is not useful as an immunohistochemical diagnostic marker for malignant course of a parathyroid tumour.

CD44. CD44 represents a family of integral cell surface glycoproteins. It is a single-span transmembrane adhesion molecule lacking kinase activity. CD44 functions by binding to its main ligand, hyaluronic acid that is abundantly present in extracellular matrix. The interaction between hyaluronic acid and ligand-binding domain of CD44 changes the conformation of the molecule and influences interaction between intracellular domains and cytoskeleton or other proteins triggering such effects as proliferation, motility and migration, adhesion and invasion. CD44 is expressed during embryonic development, on mesenchymal cells and in many cancers. It is recognised as one of the cancer stem cell markers [63, 64].

Few studies have been devoted to CD44 expression in parathyroid tumours. Focal presence of CD44 in parathyroid glands and parathyroid adenomas has been reported by Zeromski *et al*., 1998; an irregular pattern of expression was noted by this research team [65]. In contrast, absence of CD44 in normal glands has been described, and found to be statistically significantly different ($p = 0.03$) from up-regulation in hy-

perparathyroidism, observed in 48.1% of cases [15]. We found no evidence of significant CD44 expression in parathyroid tumours or tissues. Interestingly, neural-crest-derived neoplasms are CD44-negative while CD44 expression is more consistent for endoderm-derived neuroendocrine tumours [66]. Development of parathyroid glands in humans parallels the embryogenesis in mice [67] involving interaction between endoderm of the third and fourth pharyngeal pouches and the surrounding neural-crest-derived mesenchyme [68]. The interaction between mesenchyme and parathyroid epithelium [69] and molecular signalling provided by neural-crest-derived cells [70, 71] is important in parathyroid development. In addition, neural crest mesenchyme is thought to contribute directly to the formation of some cervical structures, including parathyroid glands [72] as evidenced by the unusual co-expression of Snail, Twist and E-cadherin proteins in normal and benign parathyroid glands [13].

Although CD44 has been associated with aggressive course in many malignant tumours [73, 74, 75] we did not find any expression in parathyroid carcinoma. In our experience, normal parathyroid tissues lacked CD44 as well. Thus, we conclude that CD44 has no diagnostic, prognostic or pathogenetic role in parathyroid pathology.

E-cadherin. E-cadherin is a calcium-dependent single-span transmembrane glycoprotein. It consists of extracellular domains interspersed with calcium-binding sites, a transmembrane domain and an intracellular domain. Interaction between extracellular domains ensures the intercellular adhesion mediated by E-cadherin. Intracellular domain interacts with catenins and thus is linked to cytoskeleton. This molecular chain is involved in cellular responses to mechanical forces: E-cadherin controls cell polarity, contact inhibition of cell proliferation and linkage between mechanical strain and induction of proliferation in previously quiescent cells. E-cadherin participates in cell sorting, including the processes during parathyroid embryogenesis [67, 76]. Loss of E-cadherin results in decreased cell-cell adhesion and increased ability for cell migration, invasion and metastatic spread [76, 77].

Few studies have explored E-cadherin in normal and pathological parathyroid tissues. Initially, diffuse expression of E-cadherin in parathyroid glands and adenomas was described [65]. Later, a new entity of atypical parathyroid adenoma was defined, and initial data on E-cadherin expression in parathyroid pathologies were supplemented with findings on strong membranous staining in atypical adenomas [78]. Fendrich *et al*., 2009 showed membranous expression of E-cadherin in normal and benign parathyroids, with stronger, diffuse reactivity in parathyroid tissues obtained from patients with primary (adenoma) or secondary (hyperplasia in renal failure) hyperparathyroidism. Switch to cytoplasmic pattern was evident in carcinoma [13]. Further, E-cadherin has been recently studied along with five other molecular markers in order to develop diagnostic nomogram for discrimination between benign and malignant parathyroid tumours, but there were no statistically significant differences in E-cadherin levels [79]. In our study, we demonstrated lower E-cadherin levels in proliferating parathyroid glands in comparison with normal parenchyma. As E-cadherin is involved in contact inhibition of cell proliferation, down-regulation in proliferative process is pathogenetically substantiated and supported by mild but statistically significant increase of Ki-67 expression in parathyroid hyperplasia and adenoma that was observed in the present study.

Heterogeneous expression of E-cadherin has been reported in lining of cysts within parathyroid adenomas; and in parathyroid parenchymal cells [80]. In our experience, E-cadherin showed remarkable heterogeneity. We observed both variation of staining intensity as well as hot spots leading to nodularity. Heterogeneity was lowest in normal tissues and highest in primary parathyroid hyperplasia which was in accordance with observations of Imanishi *et al*. in an animal model [50]. Clonality might limit the heterogeneity in adenomas, while epithelial mesenchymal transition might take place in carcinomas leading both to cytoplasmic displacement of E-cadherin and up-regulation of vimentin, that was observed in the current study.

CD56. Early reports pointed to absence of CD56 in parathyroid glands and their tumours [65]. Few studies have been later devoted to CD56 in parathyroid pathology; however, occasional expression by luminal membrane has been noted [80]. Our data confirm the absence of CD56 from parathyroid tissues and tumours. Thus, in controversial cases, CD56 expression in an endocrine tumour, located in the neck, would favour follicular thyroid tumour [81] but not parathyroid origin of the neoplasm. Neuroendocrine and certain haematological tumours can also feature CD56 positivity.

Interestingly, in our study adenomas were characterised by more frequent presence of perivascular nerve fibres that could indicate peculiarities of angiogenesis in primary hyperparathyroidism [82]. In hamsters, numerous nerve fibres joining the parathyroid blood vessels have been found. In these nerves, axons were located adjacent to the smooth muscle and also formed structurally specialized neuromuscular junctions with the vascular smooth muscle fibres suggesting participation in functional regulatory system [83].

CK19. Previously, invariable positivity for cytokeratin 19 has been reported in parathyroid adenomas

and carcinomas [84]. CK19 has also been found in normal parathyroid glands [85]. In our study, we succeeded to show statistically significant up-regulation of cytokeratin 19 in proliferating parathyroid lesions encompassing hyperplasia, adenoma and carcinoma. The heterogeneity was notable. As the diagnostic criteria of parathyroid carcinoma reflect invasiveness and ability to metastatic spread, the trend to up-regulation of intermediate filaments is related to the pathogenesis. In practical diagnostics, one should remember that CK19 expression is shared with thyroid pathology [86].

Vimentin. Vimentin is a major mesenchymal intermediate filament, controlling cellular motility, signalling and directional migration [87]. Previously, it has been reported that vimentin reactivity is restricted to stroma of normal parathyroid glands [85]. The published findings in adenomas are limited but controversial regarding the expression in stroma *versus* both in parenchyma and stroma [12, 85]. Expression of vimentin has been reported in parathyroid carcinoma-derived cell line exhibiting both epithelial and mesenchymal traits [88]. In the present study, we identified perinuclear, highly heterogeneous vimentin reactivity in normal parathyroid epithelium, and a trend to parenchymal up-regulation in proliferating parathyroid lesions. The expression pattern changed from perinuclear to cytoplasmic. A fraction of adenomas showed significant nodularity of vimentin expression. To the best of our knowledge, these morphological traits have not been reported previously.

Molecular heterogeneity in parathyroid tissues and tumours. Intra-tumour heterogeneity represents a hot topic in oncological research. The diversity of neoplastic cells is caused by continuous genetic changes and/or interaction with tumour microenvironment. Heterogeneity can influence the response to treatment and the survival [89, 90, 91]. It also provides basis for clonal interference that can facilitate tumour development [92]. Heterogeneity has been mostly studied in carcinomas showing fast growth and dynamic reaction to treatment [89, 90, 93, 94].

Here, we report on heterogeneity in surgically treated parathyroid adenomas and cases of primary parathyroid hyperplasia, compared to normal glands and few carcinomas. The biological nature of parathyroid pathologies precluded survival analysis as the outcome measure. Thus, descriptive morphological approach was the best way to evidence-based data in parathyroid pathology. We observed and documented significant heterogeneity regarding cell proliferation by Ki-67, cell cycle regulatory proteins p21 and cyclin D1 as well as intermediate filaments cytokeratin 19 and vimentin. The diversity can have diagnostic significance as well as pathogenetic impact on homeostasis. In diagnostics, heterogeneity influences the cut-offs and the related therapeutic decisions [95, 96]. Measurements that are performed by deliberate visual control are more likely to affected by the choice of approach: hotspot *versus* mean value, while in fully automated counting or tissue microarrays cold spots also can enter the measurable areas, influencing the results and thresholds. The hot spots clearly represent foci where certain processes, e.g., proliferation or angiogenesis, are up-regulated [97]. However, cold spots are equally important in prognostic or diagnostic aspects. In age-related macular degeneration, the abnormal deposits represent cold spots for proteolysis suggesting that impaired proteolytic degradation could be the leading pathogenetic mechanism [98]. In glioblastoma, the number of CD45-positive inflammatory cells in CD45-cold spots was an independent, significant predictor of survival advantage [99]. Thus, tissue-based parathyroid research must be appropriately designed to account for the heterogeneity, e.g., performing automated full slide immunohistochemistry, whole slide scanning and computed analysis instead of limited focal investigations and measurements. To the best of our knowledge, only few heterogeneity studies have previously been devoted to benign tumours [100, 101].

In conclusion, we have characterised the molecular profile of parathyroid glands and pathologies regarding cell proliferation and cell cycle regulation, expression of tumour suppressor proteins, adhesion molecules and intermediary filaments in an extensive tissue sample. The immunohistochemical landscape showed significant heterogeneity. Depending on the explored protein, the heterogeneity manifested as hotspots, intensity variation or changes of expression pattern.

The proliferation activity increased from baseline to primary parathyroid hyperplasia, adenoma and carcinoma. The p21 protein was significantly upregulated in PPH and adenomas. High levels of cyclin D1 were evident in PPH and carcinomas; hypothetically, overexpression of cyclin D1 could be among the driving mechanisms of increased proliferation in carcinomas, invariably lacking wild-type parafibromin. Interestingly, statistically and biologically higher levels of cyclin D1 were found in PPH than in adenomas, suggesting potential value in the differential diagnostics of these pathologies. This finding was pathogenetically justified as cyclin D1 was an early molecular driver in parathyroid pathology. Additional studies would be necessary, and correlations between cyclin D1 expression and surgical cure *versus* recurrence should be evaluated. The heterogeneity of Ki-67, p21 and cyclin D1 expression manifested as remarkable hotspot pattern. The clustering of active nuclei can have pathogenetic significance and must be accounted for in microarray-based research. However, we

showed that the mean and highest (hotspot-based) expression of Ki-67 and p21 displayed the same statistic associations. Regarding cyclin D1, only hotspot data were significantly associated with the diagnosis. Parathyroid carcinoma was characterised by loss of parafibromin, down-regulation of p27 and anti-apoptotic protein Bcl-2. Aberrant p53 protein was not found in parathyroid disease. Loss of E-cadherin, up-regulation of cytokeratin 19 and changing, heterogeneous pattern of vimentin expression was found in proliferative parathyroid lesions. CD44 and CD56 were not expressed in parathyroid glands therefore could be valuable in differential diagnostics with thyroid or other pathologies. The absence of CD44 in parathyroid carcinoma stood out against the widespread associations between CD44 and malignant tumours; however, it was well-justified by embryonal development of parathyroid glands. The remarkable heterogeneity of cell cycle markers and intermediate filaments must be accounted for in scientific studies and elaboration of diagnostic cut-offs.

Acknowledgements

We sincerely thank MD, PhD Andrejs Vanags for financial support within the frames of research project Nr. 2013/0004/1DP/1.1.1.2.0/13/APIA/VIAA/020 "Development of differential diagnostic technologies for neuroendocrine and endocrine tumours", co-financed by the European Social Fund; and MD Ilze Fridrihsone for friendly and inspiring discussions.

The authors declare no conflict of interest.

References

1. Majcen M, Hocevar M. Surgical options in treating patients with primary hyperparathyroidism. Radiol Oncol 2020; 54: 22-32.
2. Madkhali T, Alhefdhi A, Chen H, et al. Primary hyperparathyroidism. Ulus Cerrahi Derg 2016; 32: 58-66.
3. Quaglino F, Manfrino L, Cestino L, et al. Parathyroid carcinoma: an up-to-date retrospective multicentric analysis. Int J Endocrinol 2020; 2020: 7048185.
4. Nelson JA, Alsayed M, Milas M. The role of parathyroidectomy in treating hypertension and other cardiac manifestations of primary hyperparathyroidism. Gland Surg 2020; 9: 136-141.
5. Sluis K, Kim H, He Y, et al. Therapeutic challenges for elderly patients with primary hyperparathyroidism. Case Rep Endocrinol 2019; 2019: 4807081.
6. Sajid-Crockett S, Singer FR, Hershman JM. Cinacalcet for the treatment of primary hyperparathyroidism. Metabolism 2008; 57: 517-521.
7. Mizamtsidi M, Nastos C, Mastorakos G, et al. Diagnosis, management, histology and genetics of sporadic primary hyperparathyroidism: old knowledge with new tricks. Endocr Connect 2018; 7: R56-R68.
8. Rudin AV, McKenzie TJ, Wermer RA, et al. Primary hyperparathyroidism: redefining cure. Am Surg 2019; 85: 214-218.
9. DeLellis RA. Challenging lesions in the differential diagnosis of endocrine tumors: parathyroid carcinoma. Endocr Pathol 2008; 19: 221-225.
10. Do Cao C, Aubert S, Trinel C, et al. Parathyroid carcinoma: diagnostic criteria, classification, evaluation. Ann Endocrinol (Paris) 2015; 76: 165-168.
11. Gill AJ, Lim G, Cheung VKY, et al. Parafibromin-deficient (HPT-JT Type, CDC73 Mutated) parathyroid tumors demonstrate distinctive morphologic features. Am J Surg Pathol 2019; 43: 35-46.
12. Carlson D. Parathyroid pathology: hyperparathyroidism and parathyroid tumors. Arch Pathol Lab Med 2010; 134: 1639-1644.
13. Fendrich V, Waldmann J, Feldmann G, et al. Unique expression pattern of the EMT markers Snail, Twist and E-cadherin in benign and malignant parathyroid neoplasia. Eur J Endocrinol 2009; 160: 695-703.
14. Giordano TJ. Parathyroid glands. In: Rosai and Ackerman's Surgical Pathology. Goldblum JR, Lamps LW, McKenney JK, Myers JL (eds). 11th ed. Elsevier, Philadelphia 2018; 355-369.
15. Fang SH, Guidroz JA, O'Malley Y, et al. Expansion of a cell population expressing stem cell markers in parathyroid glands from patients with hyperparathyroidism. Ann Surg 2010; 251: 107-113.
16. Briede I, Strumfa I, Vanags A, et al. The association between inflammation, epithelial mesenchymal transition and stemness in colorectal carcinoma. J Inflamm Res 2020; 13: 15-34.
17. Stalhammar G, Fuentes Martinez N, Lippert M, et al. Digital image analysis outperforms manual biomarker assessment in breast cancer. Mod Pathol 2016; 29: 318-329.
18. Simtniece Z, Vanags A, Strumfa I, et al. Morphological and immunohistochemical profile of pancreatic neuroendocrine neoplasms. Pol J Pathol 2015; 66: 176-194.
19. Cetani F, Ambrogini E, Viacava P, et al. Should parafibromin staining replace HRTP2 gene analysis as an additional tool for histologic diagnosis of parathyroid carcinoma? Eur J Endocrinol 2007; 156: 547-554.
20. Cetani F, Marcocci C, Torregrossa L, et al. Atypical parathyroid adenomas: challenging lesions in the differential diagnosis of endocrine tumors. Endocr Relat Cancer 2019; 26: R441-R464.
21. Gill AJ. Understanding the genetic basis of parathyroid carcinoma. Endocr Pathol 2014; 25: 30-34.
22. Yang YJ, Han JW, Youn HD, et al. The tumor suppressor, parafibromin, mediates histone H3 K9 methylation for cyclin D1 repression. Nucleic Acids Res 2010; 38: 382-390.
23. Truran PP, Johnson SJ, Bliss RD, et al. Parafibromin, galectin-3, PGP9.5, Ki67, and cyclin D1: using an immunohistochemical panel to aid in the diagnosis of parathyroid cancer. World J Surg 2014; 38: 2845-2854.
24. Kruijff S, Sidhu SB, Sywak MS, et al. Negative parafibromin staining predicts malignant behavior in atypical parathyroid adenomas. Ann Surg Oncol 2014; 21: 426-433.
25. Juhlin CC, Haglund F, Obara T, et al. Absence of nucleolar parafibromin immunoreactivity in subsets of parathyroid malignant tumours. Virchows Arch 2011; 459: 47-53.
26. Jo JH, Chung TM, Youn H, et al. Cytoplasmic parafibromin/hCdc73 targets and destabilizes p53 mRNA to control p53-mediated apoptosis. Nat Commun 2014; 5: 5433.
27. Juhlin CC, Villablanca A, Sandelin K, et al. Parafibromin immunoreactivity: its use as an additional diagnostic marker for parathyroid tumor classification. Endocr Relat Cancer 2007; 14: 501-512.
28. Kim HK, Oh YL, Kim SH, et al. Parafibromin immunohistochemical staining to differentiate parathyroid carcinoma from parathyroid adenoma. Head Neck 2012; 34: 201-206.
29. Wang O, Wang CY, Shi J, et al. Expression of Ki-67, galectin-3, fragile histidine triad, and parafibromin in malignant and benign parathyroid tumors. Chin Med J (Engl) 2012; 125: 2895-2901.

30. Guarnieri V, Battista C, Muscarella LA, et al. CDC73 mutations and parafibromin immunohistochemistry in parathyroid tumors: clinical correlations in a single-centre patient cohort. Cell Oncol (Dordr) 2012; 35: 411-422.
31. Fernandez-Ranvier GG, Khanafshar E, Tacha D, et al. Defining a molecular phenotype for benign and malignant parathyroid tumors. Cancer 2009; 115: 334-344.
32. Rekik N, Ben Naceur B, Mnif M, et al. Hyperparathyroidism-jaw tumor syndrome: a case report. Ann Endocrinol (Paris) 2010; 71: 121-126.
33. Sun X, Kaufman PD. Ki-67: more than a proliferation marker. Chromosoma 2018; 127: 175-186.
34. Robertson S, Acs B, Lippert M, et al. Prognostic potential of automated Ki67 evaluation in breast cancer: different hot spot definitions versus true global score. Breast Cancer Res Treat 2020; 183: 161-175.
35. Wysocka J, Adamczyk A, Kruczak A, et al. High Ki-67 expression is a marker of poor survival in apocrine breast carcinoma. Pol J Pathol 2020; 71: 107-119.
36. Thomopoulou GE, Tseleni-Balafouta S, Lazaris AC, et al. Immunohistochemical detection of cell cycle regulators, Fhit protein and apoptotic cells in parathyroid lesions. Eur J Endocrinol 2003; 148: 81-87.
37. Inic Z, Inic M, Jancic S, et al. The relation between proliferation activity and parathyroid hormone levels in parathyroid tumours. J BUON 2015; 20: 562-566.
38. Abbona GC, Papotti M, Gasparri G, et al. Proliferative activity in parathyroid tumors as detected by Ki-67 immunostaining. Hum Pathol 1995; 26: 135-138.
39. Erickson LA, Jin L, Wollan P, et al. Parathyroid hyperplasia, adenomas, and carcinomas: differential expression of p27Kip1 protein. Am J Surg Pathol 1999; 23: 288-295.
40. Lumachi F, Ermani M, Marino F, et al. PCNA-LII, Ki-67 immunostaining, p53 activity and histopathological variables in predicting the clinical outcome in patients with parathyroid carcinoma. Anticancer Res 2006; 26: 1305-1308.
41. Kaczmarek E, Lacka K, Majewski P, et al. Selected markers of proliferation and apoptosis in the parathyroid lesions: a spatial visualisation and quantification. J Mol Histol 2008; 39: 509-517.
42. Demiralay E, Altaca G, Demirhan B. Morphological evaluation of parathyroid adenomas and immunohistochemical analysis of PCNA and Ki-67 proliferation markers. Turk Patoloji Derg 2011; 27: 215-220.
43. Hadar T, Shvero J, Yaniv E, et al. Expression of p53, Ki-67 and Bcl-2 in parathyroid adenoma and residual normal tissue. Pathol Oncol Res 2005; 11: 45-49.
44. Okon K, Demczuk S, Klimkowska A, et al. Correlation of microsatellite status, proliferation, apoptotic and selected immunohistochemical markers in colorectal carcinoma studied with tissue microarray. Pol J Pathol 2006; 57: 105-111.
45. Milek K, Kaczmarczyk-Sekula K, Strzepek A, et al. Mast cells influence neoangiogenesis in prostatic cancer independently of ERG status. Pol J Pathol 2016; 67: 244-249.
46. Stojadinovic A, Hoos A, Nissan A, et al. Parathyroid neoplasms: clinical, histopathological, and tissue microarray-based molecular analysis. Hum Pathol 2003; 34: 54-64.
47. Chung DC. Cyclin D1 in human neuroendocrine tumorigenesis. Ann N Y Acad Sci 2004; 1014: 209-217.
48. Qie S, Diehl JA. Cyclin D1, cancer progression, and opportunities in cancer treatment. J Mol Med (Berl) 2016; 94: 1313-1326.
49. Alao JP. The regulation of cyclin D1 degradation: roles in cancer development and the potential for therapeutic invention. Mol Cancer 2007; 6: 24.
50. Imanishi Y, Hosokawa Y, Yoshimoto K, et al. Primary hyperparathyroidism caused by parathyroid-targeted overexpression of cyclin D1 in transgenic mice. J Clin Invest 2001; 107: 1093-1102.
51. Rodriguez C, Naderi S, Hans C, et al. Parathyroid carcinoma: a difficult histological diagnosis. Eur Ann Otorhinolaryngol Head Neck Dis 2012; 129: 157-159.
52. Woodard GE, Lin L, Zhang JH, et al. Parafibromin, product of the hyperparathyroidism-jaw tumor syndrome gene HRPT2, regulates cyclin D1/PRAD1 expression. Oncogene 2005; 24: 1272-1276.
53. Juhlin C, Larsson C, Yakoleva T, et al. Loss of parafibromin expression in a subset of parathyroid adenomas. Endocr Relat Cancer 2006; 13: 509-523.
54. Bencivenga D, Caldarelli I, Stampone E, et al. p27(Kip1) and human cancers: a reappraisal of a still enigmatic protein. Cancer Lett 2017; 403: 354-365.
55. Bachs O, Gallastegui E, Orlando S, et al. Role of p27Kip1 as a transcriptional regulator. Oncotarget 2018; 9: 26259-26278.
56. Buchwald PC, Akerstrom G, Westin G. Reduced p18INK4c, p21CIP1/WAF1 and p27KIP1 mRNA levels in tumours of primary and secondary hyperparathyroidism. Clin Endocrinol (Oxf) 2004; 60: 389-393.
57. Arvai K, Nagy K, Barti-Juhasz H, et al. Molecular profiling of parathyroid hyperplasia, adenoma and carcinoma. Pathol Oncol Res 2012; 18: 607-614.
58. Cazzalini O, Scovassi AI, Savio M, et al. Multiple roles of the cell cycle inhibitor p21(CDKN1A) in the DNA damage response. Mutat Res 2010; 704: 12-20.
59. Shamloo B, Usluer S. p21 in cancer research. Cancers (Basel) 2019; 11: 1178.
60. Hassan M, Watari H, AbuAlmaaty A, et al. Apoptosis and molecular targeting therapy in cancer. Biomed Res Int 2014; 2014: 150845.
61. Naccarato AG, Marcocci C, Miccoli P, et al. Bcl-2, p53 and MIB-1 expression in normal and neoplastic parathyroid tissues. J Endocrinol Invest 1998; 21: 136-141.
62. Dabbs DJ. Diagnostic Immunohistochemistry. Theranostic and Genomic Applications. Dabbs DJ (ed.). 4th ed. Elsevier Saunders, Philadelphia 2014; 1-1008.
63. Chen C, Zhao S, Karnad A, et al. The biology and role of CD44 in cancer progression: therapeutic implications. J Hematol Oncol 2018; 11: 64.
64. Jakovlevs A, Vanags A, Gardovskis J, et al. Molecular classification of diffuse gliomas. Pol J Pathol 2019; 70: 246-258.
65. Zeromski J, Lawniczak M, Galbas K, et al. Expression of CD56/N-CAM antigen and some other adhesion molecules in various human endocrine glands. Folia Histochem Cytobiol 1998; 36: 119-125.
66. Komminoth P, Seelentag WK, Saremaslani P, et al. CD44 isoform expression in the diffuse neuroendocrine system. II. Benign and malignant tumors. Histochem Cell Biol 1996; 106: 551-562.
67. Peissig K, Condie BG, Manley NR. Embryology of the parathyroid glands. Endocrinol Metab Clin North Am 2018; 47: 733-742.
68. Chojnowski JL, Masuda K, Trau HA, et al. Multiple roles for HOXA3 in regulating thymus and parathyroid differentiation and morphogenesis in mouse. Development 2014; 141: 3697-3708.
69. Gordon J, Patel SR, Mishina Y, et al. Evidence for an early role for BMP4 signaling in thymus and parathyroid morphogenesis. Dev Biol 2010; 339: 141-154.
70. Bain VE, Gordon J, O'Neil JD, et al. Tissue-specific roles for sonic hedgehog signaling in establishing thymus and parathyroid organ fate. Development 2016; 143: 4027-4037.
71. Teshima TH, Lourenco SV, Tucker AS. Multiple cranial organ defects after conditionally knocking out Fgf10 in the neural crest. Front Physiol 2016; 7: 488.
72. Seelentag WK, Komminoth P, Saremaslani P, et al. CD44 isoform expression in the diffuse neuroendocrine system.

I. Normal cells and hyperplasia. Histochem Cell Biol 1996; 106: 543-550.
73. Zhu B, Wang Y, Wang X, et al. Evaluation of the correlation of MACC1, CD44, Twist1, and KiSS-1 in the metastasis and prognosis for colon carcinoma. Diagn Pathol 2018; 13: 45.
74. Ma J, Li M, Chai J, et al. Expression of RSK4, CD44 and MMP-9 is upregulated and positively correlated in metastatic ccRCC. Diagn Pathol 2020; 15: 28.
75. Zhou J, Du Y, Lu Y, et al. CD44 expression predicts prognosis of ovarian cancer patients through promoting epithelial-mesenchymal transition (EMT) by regulating Snail, ZEB1, and Caveolin-1. Front Oncol 2019; 9: 802.
76. Biswas KH. Molecular mobility-mediated regulation of E-cadherin adhesion. Trends Biochem Sci 2020; 45: 163-173.
77. Nagathihalli NS, Merchant NB. Src-mediated regulation of E-cadherin and EMT in pancreatic cancer. Front Biosci (Landmark Ed) 2012; 17: 2059-2069.
78. Schneider R, Bartsch-Herzog S, Ramaswamy A, et al. Immunohistochemical expression of E-cadherin in atypical parathyroid adenoma. World J Surg 2015; 39: 2477-2483.
79. Silva-Figueroa AM, Bassett R, Christakis I, et al. Using a novel diagnostic nomogram to differentiate malignant from benign parathyroid neoplasms. Endocr Pathol 2019; 30: 285-296.
80. Handra-Luca A, Tissier F. Infracentimetric parathyroid cysts in hyperparathyroidemia. Pathol Res Pract 2018; 214: 455-458.
81. Ozolins A, Narbuts Z, Strumfa I, et al. Diagnostic utility of immunohistochemical panel in various thyroid pathologies. Langenbecks Arch Surg 2010; 395: 885-891.
82. Segiet OA, Michalski M, Brzozowa-Zasada M, et al. Angiogenesis in primary hyperparathyroidism. Ann Diagn Pathol 2015; 19: 91-98.
83. Chen H, Shoumura S, Emura S. Nerve fibres in the parathyroid gland of the golden hamster (Mesocricetus auratus): immunohistochemical and ultrastructural investigations. Anat Histol Embryol 2005; 34: 34-37.
84. Li J, Chen W, Liu A. Clinicopathologic features of parathyroid carcinoma: a study of 11 cases with review of literature. Zhonghua Bing Li Xue Za Zhi 2014; 43: 296-300.
85. Miettinen M, Clark R, Lehto VP, et al. Intermediate-filament proteins in parathyroid glands and parathyroid adenomas. Arch Pathol Lab Med 1985; 109: 986-989.
86. Domagala P, Domagala W. Nuclear CK19-immunopositive pseudoinclusions as a new additional objective diagnostic feature of papillary thyroid carcinoma. Pol J Pathol 2020; 71: 1-6.
87. Cheng F, Eriksson JE. Intermediate filaments and the regulation of cell motility during regeneration and wound healing. Cold Spring Harb Perspect Biol 2017; 9: a022046.
88. Gogusev J, Murakami I, Telvi L, et al. Establishment and characterization of a human parathyroid carcinoma derived cell line. Pathol Res Pract 2015; 211: 332-340.
89. Abolins A, Vanags A, Trofimovics G, et al. Molecular subtype shift in breast cancer upon trastuzumab treatment: a case report. Pol J Pathol 2011; 62: 65-68.
90. O'Donnell RL, Kaufmann A, Weeeoodhouse L, et al. Advanced ovarian cancer displays functional intratumor heterogeneity that correlates to ex vivo drug sensitivity. Int J Gynecol Cancer 2016; 26: 1004-1011.
91. Fisher R, Pusztai L, Swanton C. Cancer heterogeneity: implications for targeted therapeutics. Br J Cancer 2013; 108: 479-485.
92. Marusyk A, Tabassum DP, Altrock PM, et al. Non-cell-autonomous driving of tumour growth supports sub-clonal heterogeneity. Nature 2014; 514: 54-58.
93. Tramm T, Kyndi M, Sorensen FB, et al. Influence of intra-tumoral heterogeneity on the evaluation of BCL2, E-cadherin, EGFR, EMMPRIN, and Ki-67 expression in tissue microarrays from breast cancer. Acta Oncol 2018; 57: 102-106.
94. Haragan A, Field JK, Davies MPA, et al. Heterogeneity of PD-L1 expression in non-small cell lung cancer: Implications for specimen sampling in predicting treatment response. Lung Cancer 2019; 134: 79-84.
95. Liszka L. Tissue heterogeneity contributes to suboptimal precision of WHO 2010 scoring criteria for Ki67 labeling index in a subset of neuroendocrine neoplasms of the pancreas. Pol J Pathol 2016; 67: 318-331.
96. Focke CM, Decker T, van Diest PJ. Intratumoral heterogeneity of Ki67 expression in early breast cancers exceeds variability between individual tumours. Histopathology 2016; 69: 849-861.
97. Biserova K, Jakovlevs A, Uljanovs R, Strumfa I. Cancer stem cells: Significance in origin, pathogenesis and treatment of glioblastoma. Cells 2021; 10: 621.
98. Leu ST, Batni S, Radeke MJ, et al. Drusen are cold spots for proteolysis: Expression of matrix metalloproteinases and their tissue inhibitor proteins in age-related macular degeneration. Exp Eye Res 2002; 74: 141-154.
99. Lipp ES, Healy P, Austin A, et al. MGMT: Immunohistochemical detection in high-grade astrocytomas. J Neuropathol Exp Neurol 2019; 78: 57-64.
100. Humphries A, Cereser B, Gay LJ, et al. Lineage tracing reveals multipotent stem cells maintain human adenomas and the pattern of clonal expansion in tumor evolution. Proc Natl Acad Sci U S A 2013; 110: E2490-E2499.
101. Mehine M, Heinonen HR, Sarvilinna N, et al. Clonally related uterine leiomyomas are common and display branched tumor evolution. Hum Mol Genet 2015; 24: 4407-4416.

Address for correspondence

Ilze Strumfa
Riga Stradins University
Latvia
e-mail: Ilze.Strumfa@rsu.lv